

## Investigation of Gas Adsorption Performances and H<sub>2</sub> Affinities of Porous Metal-Organic Frameworks with Different Entatic Metal Centers

Shengqian Ma,<sup>\*,‡</sup> Daqiang Yuan,<sup>†</sup> Jong-San Chang,<sup>§</sup> and Hong-Cai Zhou<sup>\*,†</sup>

<sup>†</sup>Department of Chemistry, Texas A&M University, P.O. Box 30012, College Station, Texas 77842, <sup>‡</sup>Chemical Sciences & Engineering Division, Argonne National Laboratory, Argonne, Illinois 60439, and <sup>§</sup>Catalysis Center for Molecular Engineering, Korea Research Institute of Chemical Technology (KRICT), Jang-dong 100, Yuseong-Gu, Daejeon 305-600, Korea

Received March 10, 2009

Three isomorphous porous metal-organic frameworks (MOFs; PCN-9 (Co/Fe/Mn)) with entatic metal centers have been constructed on the basis of the trigonal planar H<sub>3</sub>TATB ligand and a novel square-planar secondary building unit. N<sub>2</sub> adsorption isotherms at 77 K confirmed the permanent porosities of the three porous MOFs. Variable-temperature adsorption measurements of H<sub>2</sub> revealed that the H<sub>2</sub> affinities of the three porous MOFs are related to the nature of entatic metal centers, which reversely affect their H<sub>2</sub> uptake capacities.

### Introduction

Escalating research interests have in recent years been attracted to the investigation of porous metal-organic frameworks (MOFs)<sup>1</sup> for hydrogen storage applications.<sup>2</sup> In order to enhance hydrogen uptake capacities, particularly at near ambient temperatures, great efforts have been devoted to the

exploration of various strategies to increase hydrogen affinities of porous MOFs.<sup>3</sup> It has been well documented by inelastic neutron scattering (INS)<sup>4</sup> and neutron powder diffraction (NPD)<sup>5</sup> studies on porous MOFs that the inorganic metal clusters serve as the initial hydrogen adsorption sites and the metal centers have stronger interactions with the dihydrogen molecules compared to the organic linkers. In this aspect, the implementation of coordinatively unsaturated metal centers (UMCs) into porous MOFs has been considered one of the most attractive ways to improve their affinities to hydrogen.<sup>6</sup> Recent theoretical calculations suggested that the H<sub>2</sub>-open metal center interactions may be tuned by varying the metal types,<sup>7</sup> and the evaluation of

\*To whom correspondence should be addressed. E-mail: sma@anl.gov (S.M.), zhou@mail.chem.tamu.edu (H.-C.Z.).

(1) (a) Kitagawa, S.; Kitaura, R.; Noro, S.-i. *Angew. Chem., Int. Ed.* **2004**, 43, 2334. (b) Férey, G. *Chem. Soc. Rev.* **2008**, 37, 191. (c) Morris, R. E.; Wheatley, P. S. *Angew. Chem., Int. Ed.* **2008**, 47, 4966. (d) Suh, M. P.; Cheon, Y. E.; Lee, E. Y. *Coord. Chem. Rev.* **2008**, 252, 1007.

(2) (a) Pan, L.; Sander, M. B.; Huang, X.; Li, J.; Smith, M. R.; Bittner, E. W.; Bockrath, B. C.; Johnson, J. K. *J. Am. Chem. Soc.* **2004**, 126, 1308. (b) Rowsell, J. L. C.; Millward, A. R.; Park, K. S.; Yaghi, O. M. *J. Am. Chem. Soc.* **2004**, 126, 5666. (c) Millward, A. R.; Yaghi, O. M. *J. Am. Chem. Soc.* **2005**, 127, 17998. (d) Kesani, B.; Cui, Y.; Smith, M. R.; Bittner, E. W.; Bockrath, B. C.; Lin, W. *Angew. Chem., Int. Ed.* **2005**, 44, 72. (e) Sun, D.; Ke, Y.; Mattox, T. M.; Betty, A. O.; Zhou, H.-C. *Chem. Commun.* **2005**, 5447. (f) Rowsell, J. L. C.; Yaghi, O. M. *J. Am. Chem. Soc.* **2006**, 128, 1304. (g) Sun, D.; Ma, S.; Ke, Y.; Collins, D. J.; Zhou, H.-C. *J. Am. Chem. Soc.* **2006**, 128, 3896. (h) Lin, X.; Jia, J.; Zhao, X.; Thomas, K. M.; Blake, A. J.; Walker, G. S.; Champness, N. R.; Hubberstey, P.; Schröder, M. *Angew. Chem., Int. Ed.* **2006**, 45, 7358. (i) Latroche, M.; Surblé, S.; Serre, C.; Mellot-Draznieks, C.; Llewellyn, P. L.; Lee, J.-H.; Chang, J.-S.; Jung, S. H.; Férey, G. *Angew. Chem., Int. Ed.* **2006**, 45, 8227. (j) Chen, B.; Ma, S.; Zapata, F.; Lobkovsky, E. B.; Yang, J. *Inorg. Chem.* **2006**, 45, 5718. (k) Ma, S.; Sun, D.; Ambrogio, M.; Fillinger, J. A.; Parkin, S.; Zhou, H.-C. *J. Am. Chem. Soc.* **2007**, 129, 1858. (l) Ma, S.; Sun, D.; Wang, X.-S.; Zhou, H.-C. *Angew. Chem., Int. Ed.* **2007**, 46, 2458. (m) Wang, X.-S.; Ma, S. P.; Forster, M.; Yuan, D.; Eckert, J.; Lopez, J. J.; Murphy, B. J.; Parise, J. B.; Zhou, H.-C. *Angew. Chem., Int. Ed.* **2008**, 47, 7263. (n) Wang, X. S.; Ma, S.; Rauch, K.; Simmons, J. M.; Yuan, D.; Wang, X.; Yildirim, T.; Cole, W. C.; Lopez, J. J.; de Meijere, A.; Zhou, H. C. *Chem. Mater.* **2008**, 20, 3145. (o) Lin, X.; Telepeni, I.; Blake, A. J.; Dailly, A.; Brown, C. M.; Simmons, J. M.; Zoppi, M.; Walker, G. S.; Thomas, K. M.; Mays, T. J.; Hubberstey, P.; Champness, N. R.; Schröder, M. *J. Am. Chem. Soc.* **2009**, 131, 2159. (p) Ma, S.; Simmons, J. M.; Sun, D.; Yuan, D.; Zhou, H.-C. *Inorg. Chem.* **2009**, 48, DOI: 10.1021/ic900217t.

(3) (a) Rowsell, J. L. C.; Yaghi, O. M. *Angew. Chem., Int. Ed.* **2005**, 44, 4670. (b) Collins, D. J.; Zhou, H.-C. *J. Mater. Chem.* **2007**, 17, 3154. (c) Zhao, D.; Yuan, D.; Zhou, H.-C. *Energy Environ. Sci.* **2008**, 1, 222.

(4) (a) Rowsell, J. L. C.; Eckert, J.; Yaghi, O. M. *J. Am. Chem. Soc.* **2005**, 127, 14904. (b) Forster, P. M.; Eckert, J.; Heiken, B. D.; Parise, J. B.; Yoon, J. W.; Jung, S. H.; Chang, J. S.; Cheetham, A. K. *J. Am. Chem. Soc.* **2006**, 128, 16846. (c) Liu, Y.; Brown, C. M.; Neumann, D. A.; Peterson, V. K.; Kepert, C. J. *J. Alloys Compd.* **2007**, 446–447, 385. (d) Ma, S.; Eckert, J.; Forster, P. M.; Yoon, J.; Hwang, Y. K.; Chang, J.-S.; Collier, C. D.; Parise, J. B.; Zhou, H.-C. *J. Am. Chem. Soc.* **2008**, 130, 15896.

(5) (a) Yildirim, T.; Hartman, M. R. *Phys. Rev. Lett.* **2005**, 95, 215504. (b) Peterson, V. K.; Liu, Y.; Brown, C. M.; Kepert, C. J. *J. Am. Chem. Soc.* **2006**, 128, 15578. (c) Dincă, M.; Dailly, A.; Liu, Y.; Brown, C. M.; Neumann, D. A.; Long, J. R. *J. Am. Chem. Soc.* **2006**, 128, 16876. (d) Wu, H.; Zhou, W.; Yildirim, T. *J. Am. Chem. Soc.* **2007**, 129, 5314. (e) Dincă, M.; Han, W. S.; Liu, Y.; Dailly, A.; Brown, C. M.; Long, J. R. *Angew. Chem., Int. Ed.* **2007**, 46, 1419.

(6) (a) Chen, B.; Ockwig, N. W.; Millward, A. R.; Contreras, D. S.; Yaghi, O. M. *Angew. Chem., Int. Ed.* **2005**, 44, 4745. (b) Chen, B.; Zhao, X.; Putkham, A.; Hong, K.; Lobkovsky, E. B.; Hurtado, E. J.; Fletcher, A. J.; Thomas, K. M. *J. Am. Chem. Soc.* **2008**, 130, 6411. (c) Dincă, M.; Long, J. R. *Angew. Chem., Int. Ed.* **2008**, 47, 6766.

(7) (a) Sun, Y. Y.; Kim, Y.-H.; Zhang, S. B. *J. Am. Chem. Soc.* **2007**, 129, 12606. (b) Zhou, W.; Wu, H.; Yildirim, T. *J. Am. Chem. Soc.* **2008**, 130, 15268.

different UMCs' affinities to hydrogen molecules will be very instructive for the future design of porous MOFs with high hydrogen adsorption capacities, especially at near ambient temperatures. Although the influence of cation exchange on hydrogen adsorption of porous MOFs has been recently reported,<sup>8</sup> systematic investigation of hydrogen affinities of different UMCs, which usually requires the construction of isomorphous structures with different metal atoms, has rarely been performed.<sup>7b</sup>

Recently, we reported a biomimetic approach to achieving UMCs by creating entatic metal centers with a similar configuration to the active iron center of hemoglobin (Figure 1a) in PCN-9 (Co) (PCN represents porous coordination network).<sup>9</sup> PCN-9 (Co) adopts a square-planar secondary building unit (SBU; Figure 1b) which contains four hemoglobin-like entatic cobalt centers bundled through sharing a  $\mu_4$ -oxo bridge and exhibits high affinity to dihydrogen molecules. Herein, we extend this strategy to other metal systems and obtain two new porous MOFs designated as PCN-9 (Fe) and PCN-9 (Mn), which are isostructural with PCN-9 (Co) but contain entatic iron and manganese centers, respectively. In this contribution, we present their detailed structural analysis together with their N<sub>2</sub> and H<sub>2</sub> sorption performances as well as a systematic evaluation of entatic Co, Fe, and Mn centers' affinities to dihydrogen molecules.

## Experimental Section

**Synthesis of PCN-9 (Co).**<sup>9</sup> A mixture of the H<sub>3</sub>TATB ligand (0.01 g,  $2.26 \times 10^{-5}$  mol) and Co(NO<sub>3</sub>)<sub>2</sub>·6H<sub>2</sub>O (0.025 g,  $8.6 \times 10^{-5}$  mol) together with six drops of dimethylformamide (DMF) and three drops of HBF<sub>4</sub> (50% aqua solution) in 1.2 mL of dimethylsulfoxide (DMSO) was sealed in a Pyrex glass tube (i.d. 8 mm/o.d. 10 mm) and heated to 135 °C at a rate of 1 °C/min. After staying at 135 °C for 72 h, it was cooled to 35 °C at a rate of 0.1 °C/min. The resulting violet crystals were washed with DMSO twice to give pure PCN-9 (Co<sub>4</sub>O(TATB)<sub>8/3</sub>·2H<sub>3</sub>O<sup>+</sup>·5H<sub>2</sub>O·8DMSO, yield: 55%). The reaction was amplified to gram quantity using multiple tubes. Elem anal. calcd for PCN-9 (Co): C, 44.20%; H, 4.45%; N, 5.15%. Found: C, 44.19%; H, 4.51%; N, 5.16%.

**Synthesis of PCN-9 (Fe).** A mixture of the H<sub>3</sub>TATB ligand (0.01 g,  $2.26 \times 10^{-5}$  mol) and FeCl<sub>2</sub> (0.02 g,  $1.58 \times 10^{-4}$  mol) together with six drops of DMF and three drops of HBF<sub>4</sub> (50% aqua solution) in 1.2 mL of DMSO was first put into a Pyrex glass tube (i.d. 8 mm/o.d. 10 mm) in a glovebox under a nitrogen atmosphere and then sealed by freezing the tube with liquid nitrogen. The sealed tube was heated to 135 °C at a rate of 1 °C/min. After staying at 135 °C for 72 h, it was cooled to 35 °C at a rate of 0.1 °C/min. The resulting dark red crystals were washed with DMSO twice in the glovebox to give pure PCN-9 (Fe) (Fe<sub>4</sub>O(TATB)<sub>8/3</sub>·5H<sub>2</sub>O·10DMSO, yield: 50%). The reaction was amplified to gram quantity using multiple tubes. Elem anal. calcd for PCN-9 (Fe): C, 44.25%; H, 4.51%; N, 4.91%. Found: C, 42.01%; H, 4.45%; N, 4.84%.

**Synthesis of PCN-9 (Mn).** A mixture of the H<sub>3</sub>TATB ligand (0.01 g,  $2.26 \times 10^{-5}$  mol), Mn(ClO<sub>4</sub>)<sub>2</sub>·6H<sub>2</sub>O (0.015 g,  $5.17 \times 10^{-5}$  mol), and Mn(CH<sub>3</sub>COO)<sub>3</sub>·2H<sub>2</sub>O (0.015 g,  $5.6 \times 10^{-5}$  mol) in 1.2 mL of DMSO was sealed in a Pyrex glass tube (i.d. 8 mm/o.d. 10 mm) and heated to 135 °C at a rate of 1 °C/min. After staying at 135 °C for 72 h, it was cooled to 35 °C at a rate of 0.1 °C/min. The resulting brown crystals were

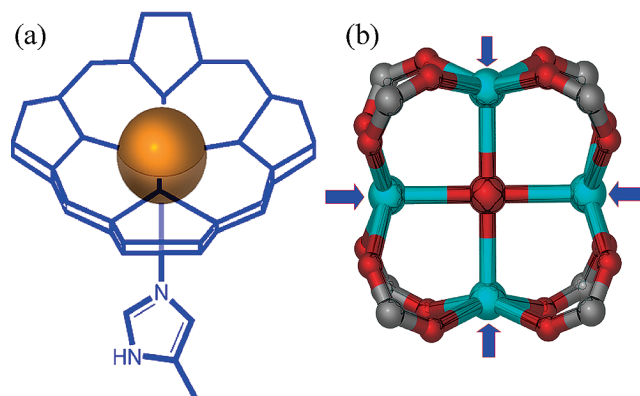


**Figure 1.** (a) The active center of hemoglobin (the orange sphere represents an Fe atom). (b) The M<sub>4</sub>( $\mu_4$ -O)(carboxylate)<sub>4</sub> SBU, with arrows indicating the displaced entatic metal centers (M = Co, Fe, Mn). Color scheme: C, gray; M, aqua; and O, red.

washed with DMSO twice to give pure PCN-9 (Mn) (Mn<sub>4</sub>O(TATB)<sub>8/3</sub>·2H<sub>3</sub>O<sup>+</sup>·5H<sub>2</sub>O·8DMSO, yield: 60%). The reaction was amplified to gram quantity using multiple tubes. Elem anal. calcd for PCN-9 (Mn): C, 44.06%; H, 4.71%; N, 4.67%. Found: C, 42.61%; H, 4.41%; N, 4.37%.

**Single-Crystal X-Ray Crystallography.** Single-crystal X-ray data were collected on a Bruker Smart Apex diffractometer equipped with an Oxford Cryostream low-temperature device and a fine-focus sealed-tube X-ray source (Mo K $\alpha$  radiation,  $\lambda = 0.71073$  Å, graphite monochromated) operating at 45 kV and 35 mA. The crystals were protected with Paratone oil from the air and moisture and mounted on the tip of a glass fiber of a goniometer. Frames were collected with 0.3° intervals in the  $\varphi$  and  $\omega$  modes for 30 s per frame such that a hemisphere of data was collected. Raw data collection and refinement were done using SMART. Data reduction was performed using SAINT+ and corrected for Lorentz and polarization effects.<sup>10</sup> The structure was solved by direct methods and refined by full-matrix least-squares on  $F^2$  with anisotropic displacement using SHELX-97.<sup>11</sup> Non-hydrogen atoms were refined with anisotropic displacement parameters during the final cycles. Hydrogen atoms on carbon were calculated in ideal positions with isotropic displacement parameters set to  $1.2 \times U_{eq}$  of the attached atom. In all cases, solvent molecules were highly disordered, and attempts to locate and refine the solvent peaks were unsuccessful. Contributions to scattering due to these solvent molecules were removed using the SQUEEZE routine of PLATON and refined further using the data generated.<sup>12</sup>

**Low-Pressure Gas Adsorption Measurements.** Low-pressure gas adsorption measurements were measured with a Beckman Coulter SA 3100 surface area and pore size analyzer. A sample was soaked with methanol for 24 h, and the extract was discarded. Fresh methanol was subsequently added, and the crystals were allowed to soak for another 24 h to remove DMSO and H<sub>2</sub>O solvates. The sample was then treated with dichloromethane similarly to remove methanol solvates. For PCN-9 (Fe), these procedures were performed in a glovebox under a nitrogen atmosphere. After the removal of dichloromethane by decanting, the sample was dried under a dynamic vacuum ( $< 10^{-3}$  torr) at room temperature (25 °C) overnight. Before gas adsorption measurement, the sample was dried again by using the "outgas" function of the surface area analyzer for 1 h at 60 °C. A sample of 100.0 mg was used for N<sub>2</sub> adsorption

(10) SAINT+, version 6.22; Bruker Analytical X-Ray Systems, Inc.: Madison, WI, 2001.

(11) Sheldrick, G. M. SHELX-97; Bruker Analytical X-Ray Systems, Inc.: Madison, WI, 1997.

(12) Spek, A. L. *J. Appl. Crystallogr.* **2003**, *36*, 7.

(8) (a) Dincă, M.; Long, J. R. *J. Am. Chem. Soc.* **2007**, *129*, 11172. (b) Mulfort, K. L.; Hupp, J. T. *Inorg. Chem.* **2008**, *47*, 7936.

(9) Ma, S.; Zhou, H.-C. *J. Am. Chem. Soc.* **2006**, *128*, 11734.

**Table 1.** Crystal Data<sup>a</sup> and Structure Refinement of PCN-9 (Co), PCN-9 (Fe), and PCN-9 (Mn)

	PCN-9 (Co)	PCN-9 (Fe)	PCN-9 (Mn)
formula	Co <sub>4</sub> C <sub>64</sub> H <sub>32</sub> N <sub>8</sub> O <sub>17</sub>	Fe <sub>4</sub> C <sub>64</sub> H <sub>32</sub> N <sub>8</sub> O <sub>17</sub>	Mn <sub>4</sub> C <sub>64</sub> H <sub>32</sub> N <sub>8</sub> O <sub>17</sub>
fw	1420.70	1408.38	1404.74
crystal system	cubic	cubic	cubic
space group	<i>Im</i> $\bar{3}m$	<i>Im</i> $\bar{3}m$	<i>Im</i> $\bar{3}m$
cryst size (mm)	0.16 × 0.12 × 0.10	0.11 × 0.09 × 0.08	0.21 × 0.16 × 0.14
<i>a</i> , Å	25.4387(5)	25.474(3)	25.5155(6)
<i>b</i> , Å	25.4387(5)	25.474(3)	25.5155(6)
<i>c</i> , Å	25.4387(5)	25.474(3)	25.5155(6)
$\alpha$ , deg	90.00	90.00	90.00
$\beta$ , deg	90.00	90.00	90.00
$\gamma$ , deg	90.00	90.00	90.00
<i>V</i> , Å <sup>3</sup>	16462(1)	16531(3)	16611 (6)
<i>Z</i>	6	6	6
<i>d</i> <sub>calc</sub> , g cm <sup>-3</sup>	0.860	0.849	0.843
GOF	1.218	1.087	1.306
<i>R</i> <sub>1</sub> , <i>wR</i> <sub>2</sub> <sup>b</sup>	0.1031, 0.307	0.1315, 0.3338	0.1484, 0.3614

<sup>a</sup> Obtained with graphite-monochromated Mo K $\alpha$  ( $\lambda = 0.71073$  Å) radiation. <sup>b</sup>  $R_1 = \sum ||F_o| - |F_c|| / \sum |F_o|$  and  $wR_2 = \{[\sum w(F_o^2 - F_c^2)^2] / [\sum w(F_o^2)^2]\}^{1/2}$ .

**Table 2.** Gas Adsorption Summary of PCN-9 (Co), PCN-9 (Fe), and PCN-9 (Mn)

	BET surface area (m <sup>2</sup> /g)	Langmuir surface area (m <sup>2</sup> /g)	pore volume (cm <sup>3</sup> /g)	H <sub>2</sub> uptake (wt %, at 77 K, 760 Torr)	isosteric heats of adsorption ( <i>Q</i> <sub>st</sub> ) at low H <sub>2</sub> coverage (kJ/mol)
PCN-9 (Co)	1064 ± 26	1355 ± 33	0.51 ± 0.01	1.53 ± 0.10	10.1
PCN-9 (Fe)	682 ± 18	848 ± 22	0.33 ± 0.01	1.06 ± 0.03	6.4
PCN-9 (Mn)	836 ± 29	1057 ± 37	0.41 ± 0.02	1.26 ± 0.05	8.7

measurement and was maintained at 77 K with liquid nitrogen. In the hydrogen storage measurement, high-purity hydrogen (99.9995%) and an 80.0 mg sample were used. The regulator and pipe were flushed with hydrogen before being connected to the analyzer. The internal lines of the instrument were flushed three times by utilizing the “flushing lines” function of the program to ensure the purity of H<sub>2</sub>. The measurement was maintained at 77 K with liquid nitrogen. The temperature at 87 K was maintained with a liquid argon bath. (All of the measured sorption isotherms have been repeated five times to confirm the reproducibility within experimental error, and standard deviation numbers are enumerated in Table 2.)

## Results and Discussion

**Structural Description.** Single-crystal X-ray analysis revealed that the three MOFs are isostructural with each other, crystallizing in the *Im* $\bar{3}m$  space group (Table 1). They all adopt the square-planar M<sub>4</sub>( $\mu_4$ -O) SBU (M = Co, Fe, Mn), with the  $\mu_4$ -O residing at the center of the square of four M atoms (Figure 1b). All four of the M atoms in the SBU are in the same plane and coordinate five oxygen atoms (four from four carboxylate groups of four different TATB ligands and one from the  $\mu_4$ -O) with square-pyramidal geometry. The M– $\mu_4$ -O distance is 2.351(2) Å for Co, 2.313 (3) Å for Fe, and 2.194 (3) Å for Mn. If one of the five-coordinate M atoms is compared to the active Fe center in hemoglobin (Figure 1a), the  $\mu_4$ -O is analogous to the proximal ligand, and on the opposite side of the square-pyramidal base is the distal position of the M, which is below the plane of the four O atoms in an entatic state and ready to bind a substrate to achieve octahedral coordination.

There exist two types of cages in their structures: one is a truncated octahedral cage defined by six M<sub>4</sub>( $\mu_4$ -O) SBUs at the corners and eight TATB ligands on the faces (Figure 2a), and the other one is a cuboctahedral cage

enclosed by eight truncated octahedral cages occupying the vertices of the cube (Figure 2b). Every cuboctahedral cage connects eight truncated octahedral cages via face-sharing, and each truncated octahedral cage links six cuboctahedral cages to form an (8,3)-net framework (Figure 3a). Two such (8,3)-nets are mutually interpenetrated due to the  $\pi$ – $\pi$  interactions (Table 2) of the TATB ligand pairs (Figure 3b), with the second being generated through translation along [110].<sup>13</sup> The staggered TATB ligand pairs resulting from strong  $\pi$ – $\pi$  interactions lead to the truncated octahedral cages of one set framework enclosed by the cuboctahedral cages of the other set framework with triangular face-sharing (Figure 2c). This closes the windows of the truncated octahedral cages and also reduces the size of the opening of the cuboctahedral cages, resulting in  $\sim 5 \times 5$  Å square pores with all entatic metal centers open toward channels ready for gas substrates to bind.

**Gas Sorption Studies.** To test the permanent porosities of the three porous MOFs, N<sub>2</sub> sorption isotherms were measured at 77 K for the samples that were activated according to the procedures in the Experimental Section. As shown in Figure 4, all of them exhibit type-I sorption behavior, as expected for microporous materials. Derived from the N<sub>2</sub> sorption data, the BET surface areas are 1064 m<sup>2</sup>/g (Langmuir surface area, 1355 m<sup>2</sup>/g), 682 m<sup>2</sup>/g (Langmuir surface area, 848 m<sup>2</sup>/g), and 836 m<sup>2</sup>/g (Langmuir surface area, 1057 m<sup>2</sup>/g) for PCN-9 (Co), PCN-9 (Fe), and PCN-9 (Mn), respectively, and the total pore volume is 0.51 cm<sup>3</sup>/g for PCN-9 (Co), 0.33 cm<sup>3</sup>/g for PCN-9 (Fe), and 0.41 cm<sup>3</sup>/g for PCN-9 (Mn) (Table 2).

(13) (a) Ma, S.; Wang, X.-S.; Yuan, D.; Zhou, H.-C. *Angew. Chem., Int. Ed.* **2008**, *47*, 4130. (b) Ma, S.; Yuan, D.; Wang, X.-S.; Zhou, H.-C. *Inorg. Chem.* **2009**, *48*, 2072.

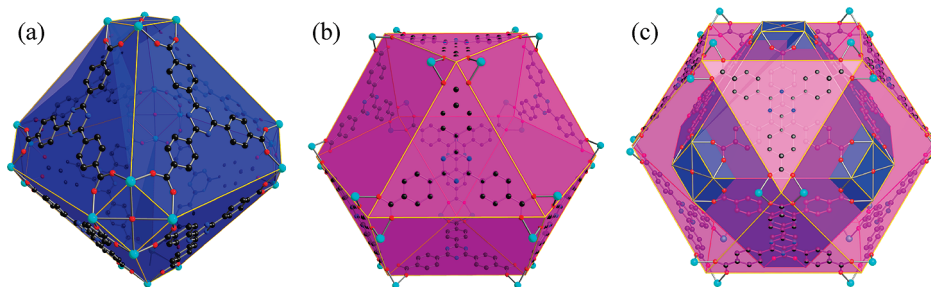


**Figure 2.** (a) Truncated octahedral cage. (b) Cuboctahedral cage. (c) An octahedral cage enclosed by a cuboctahedral cage from another network.

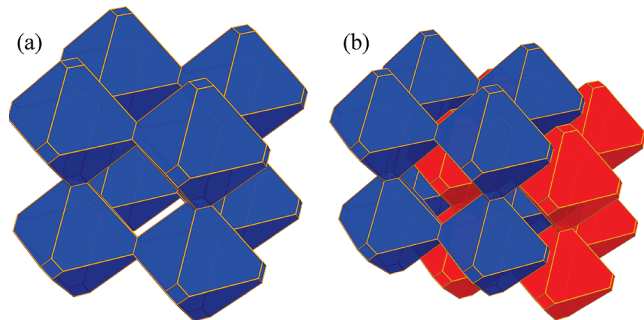


**Figure 3.** (a) Single (8,3)-connected net formed by corner-sharing of octahedral cages. (b) Doubly interpenetrated (8,3)-connected nets resulted from  $\pi$ - $\pi$  interactions of the TATB ligand pairs.

$H_2$  sorption measurements at 77 K were also carried out to check their hydrogen storage performances. As indicated in Figure 5, at 77 K and 760 Torr, the hydrogen uptake capacity of PCN-9 (Co) is 1.53 wt %, and PCN-9 (Fe) can adsorb 1.06 wt % hydrogen, while PCN-9 (Mn) can uptake 1.26 wt % hydrogen (Table 2). Those values are relatively lower compared to some reported porous MOFs with much higher surface areas.<sup>2,4</sup>

The hydrogen adsorption performances of the three porous MOFs are almost proportional with their surface areas, the difference of which can be presumably due to the degree of sample activation, possibly as a result of different metal-center-guest-solvent interactions, together with appreciably different pore sizes originating from the radii of three metal ions, and similar phenomena have been observed in other isostructural MOFs.<sup>5c,5e</sup>

**Analysis of Gas Affinities.** The gas affinities of porous MOFs can be quantitatively reflected by isosteric heats of adsorption  $Q_{st}$ , which are calculated utilizing the Clausius-Clapeyron equation,<sup>14</sup> using isotherms measured at different temperatures.

$$Q_{st} = -R d(\ln P)/d(1/T)$$

To estimate the  $H_2$  affinities of the three porous MOFs,  $H_2$  adsorption isotherms at 77 and 87 K were collected for the calculation of their  $Q_{st}$  (Figure S1–S3, Supporting Information). As indicated in Figure 6, the  $Q_{st}$  of hydrogen adsorbed in all three PCN-9s decreases with the increase of hydrogen loadings, which is similar to those observed in other porous MOFs.<sup>2f,2i,2n,4b,4d,5c,5e,8a</sup> The

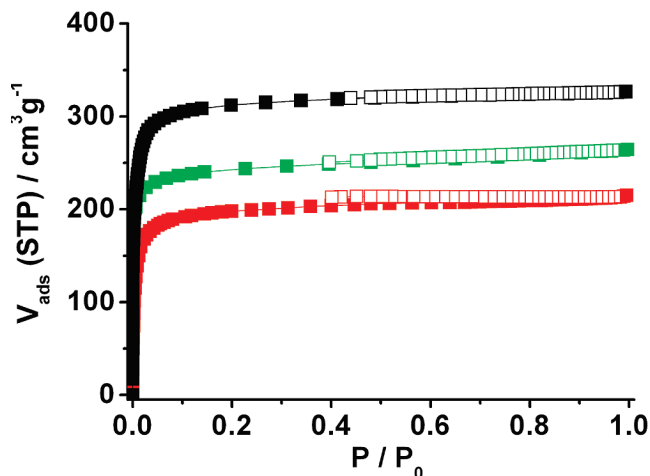


**Figure 4.**  $N_2$  sorption isotherms of PCN-9s at 77 K (black symbol, Co; red symbol, Fe; green symbol, Mn; solid square, adsorption; open square, desorption).

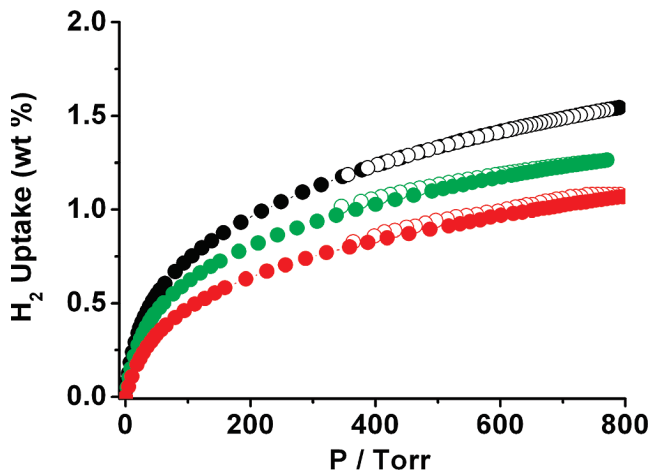


**Figure 5.**  $H_2$  sorption isotherms of PCN-9s at 77 K (black symbol, Co; red symbol, Fe; green symbol, Mn; solid circle, adsorption; open circle, desorption).

average  $Q_{st}$  of PCN-9 (Co) is about 2 kJ/mol higher than that of PCN-9 (Mn) and is around 3 kJ/mol higher compared to that of PCN-9 (Fe). At low hydrogen coverage, which can be assumed as  $H_2$ -open metal center interactions, as suggested by recent INS and NPD studies,<sup>4,5</sup> PCN-9 (Co) has a  $Q_{st}$  of 10.1 kJ/mol and PCN-9 (Mn) has a  $Q_{st}$  of 8.7 kJ/mol, while PCN-9 (Fe) has a relatively lower  $Q_{st}$  of 6.4 kJ/mol. This indicates that, among Co, Mn, and Fe, the entatic Co center has the highest affinity to dihydrogen molecules, while entatic Fe has the lowest.

(14) (a) Roquerol, F.; Rouquerol, J.; Sing, K. *Adsorption by Powders and Solids: Principles, Methodology, and Applications*; Academic Press: London, 1999. (b) Ma, S.; Sun, D.; Simmons, J. M.; Collier, C. D.; Yuan, D.; Zhou, H.-C. *J. Am. Chem. Soc.* 2008, 130, 1012.

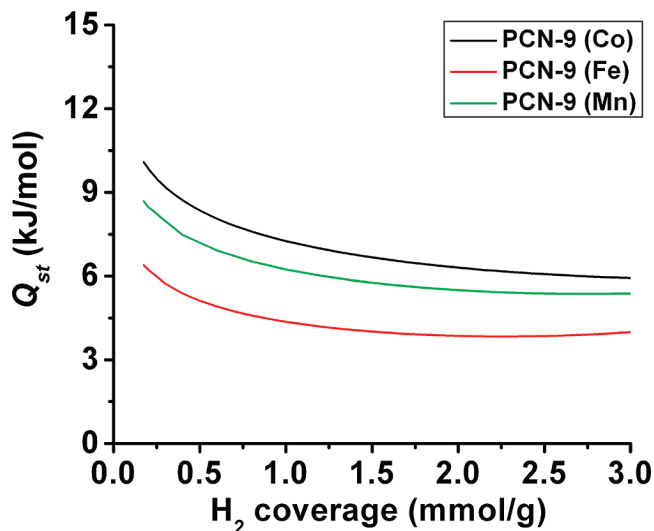


Figure 6. Isosteric heats of adsorption of H<sub>2</sub> in PCN-9s.

The different hydrogen affinities of the three entatic metal centers can be qualitatively understood on the basis of their coordination preferences,<sup>7b</sup> which usually follow the empirical, Irving–Williams sequence (i.e., “Mn<sup>2+</sup> < Fe<sup>2+</sup> < Co<sup>2+</sup> < Ni<sup>2+</sup> < Cu<sup>2+</sup> > Zn<sup>2+</sup>”).<sup>15</sup> The observed lower  $Q_{st}$  of PCN-9 (Fe) compared to that of PCN-9 (Mn) can be attributed to partial oxidation of Fe<sup>2+</sup> to Fe<sup>3+</sup> in PCN-9 (Fe), as evidenced by Mössbauer studies (Figure S6, Supporting Information). The trend of H<sub>2</sub> binding found here is also consistent with the findings from a recent study on hydrogen adsorption in

isostructural MOFs with different liberated open metal sites.<sup>7b</sup>

## Conclusions

In summary, three isostructural porous MOFs based on the novel square-planar SBU with entatic Co, Fe, and Mn centers for PCN-9 (Co), PCN-9 (Fe), and PCN-9 (Mn), respectively, have been constructed and structurally characterized. Nitrogen sorption measurements at 77 K confirmed the permanent porosities of the three porous MOFs. Hydrogen sorption studies revealed that the entatic Co center possesses a higher hydrogen affinity compared to the entatic Fe and Mn centers, indicating that the implementation of open Co centers into porous MOFs may be a promising way to enhance hydrogen adsorption enthalpies for near-ambient hydrogen storage application. This aspect of the work is being undergone in our lab.

**Acknowledgment.** This work was supported by the U.S. Department of Energy (DEFC36-07GO17033 to H.-C.Z.) and the National Science Foundation (CHE-0449634 to H.-C.Z.). S.M. acknowledges the Director’s Postdoctoral Fellowship from Argonne National Laboratory and thanks Dr. Tom Scott for Mössbauer measurements. J.-S.C. is grateful to KOI through the Institutional Research Program (KK-0904-A0) for the financial support.

**Supporting Information Available:** Crystallographic information files (CIF) of PCN-9 (Fe/Mn), hydrogen adsorption isotherms of PCN-9 (Co/Fe/Mn) at 87 K, a structure picture, and the Mössbauer spectrum of PCN-9 (Fe) are available free of charge via the Internet at <http://pubs.acs.org>.

(15) Irving, H.; Williams, R. J. *Nature* **1948**, *162*, 146.